



## Geophysical Research Letters



#### RESEARCH LETTER

10.1029/2023GL106760

#### **Key Points:**

- Multidisciplinary Drifting Observatory for the Study of Arctic Climate observations enable improved thermodynamic process understanding and representation in sea ice models
- Resolved meter-scale ice and snow thickness heterogeneity and horizontal heat conduction enhance conductive heat flux by up to 10% in models
- A positive surface temperature model bias up to 5 K suggests a misrepresentation of the surface energy balance over thin ice

#### **Supporting Information:**

Supporting Information may be found in the online version of this article.

#### Correspondence to:

L. Zampieri, lorenzo.zampieri@cmcc.it

#### Citation:

Zampieri, L., Clemens-Sewall, D., Sledd, A., Hutter, N., & Holland, M. (2024). Modeling the winter heat conduction through the sea ice system during MOSAiC. *Geophysical Research Letters*, 51, e2023GL106760. https://doi.org/10.1029/2023GL106760

Received 9 OCT 2023 Accepted 3 APR 2024

# © 2024. The Authors. This is an open access article under the terms of the Creative Commons Attribution License, which permits use, distribution and reproduction in any medium, provided the original work is properly cited.

## Modeling the Winter Heat Conduction Through the Sea Ice System During MOSAiC

Lorenzo Zampieri<sup>1,2</sup>, David Clemens-Sewall<sup>2</sup>, Anne Sledd<sup>3,4</sup>, Nils Hutter<sup>5,6</sup>, and Marika Holland<sup>2</sup>

<sup>1</sup>Now at CMCC Foundation—Euro-Mediterranean Center on Climate Change, Bologna, Italy, <sup>2</sup>National Center for Atmospheric Research, Boulder, CO, USA, <sup>3</sup>Cooperative Institute for Research in Environmental Sciences, University of Colorado Boulder, Boulder, CO, USA, <sup>4</sup>National Oceanic and Atmospheric Administration Physical Sciences Laboratory, Boulder, CO, USA, <sup>5</sup>Cooperative Institute of Climate, Ocean and Ecosystem Studies (CICOES), University of Washington, Seattle, WA, USA, <sup>6</sup>Alfred-Wegener-Institut, Helmholtz-Zentrum für Polar- und Meeresforschung, Bremerhaven, Germany

**Abstract** Models struggle to accurately simulate observed sea ice thickness changes, which could be partially due to inadequate representation of thermodynamic processes. We analyzed co-located winter observations of the Arctic sea ice from the Multidisciplinary Drifting Observatory for the Study of the Arctic Climate for evaluating and improving thermodynamic processes in sea ice models, aiming to enable more accurate predictions of the warming climate system. We model the sea ice and snow heat conduction for observed transects forced by realistic boundary conditions to understand the impact of the non-resolved meterscale snow and sea ice thickness heterogeneity on horizontal heat conduction. Neglecting horizontal processes causes underestimating the conductive heat flux of 10% or more. Furthermore, comparing model results to independent temperature observations reveals a ~5 K surface temperature overestimation over ice thinner than 1 m, attributed to shortcomings in parameterizing surface turbulent and radiative fluxes rather than the conduction. Assessing the model deficiencies and parameterizing these unresolved processes is required for improved sea ice representation.

Plain Language Summary Numerical sea ice models rely on conceptual simplifications of the sea ice and snow conditions observed in the Arctic and Southern Ocean. In particular, we cannot account for the variations in sea ice thickness and snow depth at the meter scale because we have limited computing capabilities and lack a detailed understanding of the processes defining how the sea ice system evolves. Furthermore, when designing sea ice models, we assume that the heat can flow only vertically, while in reality, this exchange is also horizontal and depends on the local topography. Thanks to observations collected during the Multidisciplinary Drifting Observatory for the Study of Arctic Climate expedition, we can better quantify model errors when using thermodynamic approximations. Our findings suggest that slightly more heat flows through the sea ice system than we can simulate with a simplified sea ice model and that the surface temperature of the model is too warm for thin ice and snow conditions. Learning the nature of these errors is useful because we could formulate corrections for our models, investigate the occurrence of climate feedback mechanisms, and possibly provide more reliable predictions about the current state of the sea ice and its future evolution, which is currently heavily impacted by global warming.

#### 1. Introduction

The sea ice is a complex system that exhibits substantial heterogeneity in terms of its composition, which includes ice, precipitated snow, and pockets of brine and air within the ice (Weeks & Assur, 1967). Consequently, the material and thermodynamic properties of the system are also heterogeneous, with substantial spatiotemporal density and thermal conductivity variations (Jutila et al., 2022; Timco & Frederking, 1996). Small-scale heterogeneity is manifested also in terms of the sea ice thickness, with the coexistence of thin level ice and thick pressure ridges at the scale of tens of meters (Thorndike et al., 1975; von Albedyll et al., 2021). Ridges cover 25%–45% of the total sea ice area (Mårtensson et al., 2012), and they favor preferential snow accumulation in their vicinity (Macfarlane, Schneebeli, et al., 2023), thus inducing snow heterogeneity. During winter, the temperature difference between the ocean and the atmosphere typically favors upward heat conduction through the sea ice and snow. While often conceptualized as vertical and thus one-dimensional, this thermodynamic process is in reality

three-dimensional. The exact pathway of the heat dissipation through sea ice and snow is set by the system's small-scale geometry and thermal conductivity. In this context, the role of snow on sea ice is of particular importance because this material is a strong thermal insulator with a thermal conductivity approximately one order of magnitude smaller than that of sea ice (Schwerdtfecer, 1963; Sturm et al., 1997). Therefore, the spatial distribution of the snow over sea ice and its depth variations could have first-order implications for winter heat conduction.

Sea ice models run at resolutions as fine as a few kilometers, which is insufficient for explicitly capturing the observed topographic heterogeneity manifested at the meter scale. Several models now feature a prognostic subgrid discretization in multiple ice thickness classes, which provide a coarse statistical description of the sea ice thickness heterogeneity and, to a certain extent, of the snow precipitating on it (Holland et al., 2006; Lipscomb, 2001; Massonnet et al., 2019; Thorndike et al., 1975). We call this model formulation the Ice Thickness Distribution (ITD). While the snow is also discretized prognostically at the subgrid scale following the ITD, complex snow processes such as snow redistribution and metamorphism are not considered in thermodynamics computations (Clemens-Sewall et al., 2022). The consequence of omitting these processes is that the model representation of ice and snow lacks topographic heterogeneity (Fichefet & Maqueda, 1997) and, typically, the heat conduction can be solely represented as a vertical process, thus neglecting its horizontal components. To our knowledge, only a few studies tried to quantify this model deficiency. Petrich et al. (2007) discuss how lateral ice growth impacts the healing of ice cracks at very fine spatial scale. Sturm, Perovich, and Holmgren (2002) indicated a 40% underestimation of the heat conduction based on a single 60 m transect measured during the Surface Heat Budget of the Arctic Ocean (SHEBA) observational campaign (D. K. Perovich et al., 1999; Sturm, Holmgren, & Perovich, 2002). He suggests increasing the model snow conductivity k<sub>s</sub> from the observed bulk value of 0.14 W m<sup>-1</sup> K<sup>-1</sup> to an effective value of 0.2 W m<sup>-1</sup> K<sup>-1</sup> to compensate for the unresolved horizontal conduction. In addition, they argue that  $k_s$  should be increased to higher values when considering buoyancydriven air convection within snow. Note that the quality needle probe  $k_s$  measurement technique used by Sturm, Perovich, and Holmgren (2002) has been questioned by Riche and Schneebeli (2013). Popović et al. (2020) found no imprint of the small-scale snow heterogeneity on the horizontal heat conduction when considering the sea ice thickness to be constant, an assumption appropriate for level ice but not adequate for the deformed parts of the domain.

Localized measurements of snow thermal conductivity span a considerable range due to their dependency on the physical properties of the snow (e.g., temperature, grain characteristics, and bonding) and differences in measuring techniques. Consequently, observed values for  $k_s$  are from about 0.03 to 0.65 W m<sup>-1</sup> K<sup>-1</sup> (Sturm et al., 1997). During the Multidisciplinary Drifting Observatory for the Study of Arctic Climate (MOSAiC) expedition (Nicolaus et al., 2022; Shupe et al., 2022), the observed k, range was typically lower when considering vertical averages over accumulated snow layers (e.g., from 0.2 to 0.3 W m<sup>-1</sup> K<sup>-1</sup> in Macfarlane, Löwe, et al. (2023)). Indirect MOSAiC k<sub>s</sub> estimates based on Snow and Ice Mass Balance Array (SIMBA hereafter) buoy data suggest higher values for this parameter ( $k_s = 0.41 \text{ W m}^{-1} \text{ K}^{-1}$ ; D. Perovich et al., 2023). Snow density changes cause k<sub>n</sub> to increase in winter until March, and decrease afterward (Macfarlane, Löwe, et al., 2023). Despite the observed  $k_s$  range, we still typically assume the snow thermal conductivity to be a constant in largescale sea ice models, and only Lecomte et al. (2013) attempted to develop a wind-driven parameterization for this parameter. Moreover, the snow thermal conductivity is often used as a tuning knob to enhance or suppress the winter sea ice growth (Urrego-Blanco et al., 2016; Zampieri et al., 2021). This tuning approach is effective in obtaining the wanted result, which is improved sea ice simulations in terms of the pan-Arctic sea ice extent and volume. Whether such tuning is appropriate also in terms of small-scale thermodynamic processes and compatible with the available sea ice observations remains an open question. Setting better physical boundaries for thermodynamic tuning could help to obtain more accurate Arctic and Antarctic sea ice projections, given the expected relevance of snow processes in a warming climate (Landrum & Holland, 2022).

Here, we revisit and expand the result of Sturm, Perovich, and Holmgren (2002) in the context of sea ice and snow observations collected during the MOSAiC expedition in the winter of 2019–2020 and in light of the advances made by the sea ice modeling community in the last two decades. The scientific questions we address in this study are the following:

1. In sea ice models, what is the effect of the unresolved snow and ice thickness heterogeneity on the conductive heat flux?

ZAMPIERI ET AL. 2 of 11

- 2. What is the effect of modeling the conduction as a two-dimensional process?
- 3. How do these effects vary across diverse sea ice types with different thicknesses?
- 4. Can an equilibrium thermodynamic model of sea ice reproduce the MOSAiC temperature observations?
- 5. Is tuning the snow thermal conductivity compatible with small-scale thermodynamic-oriented diagnostics?

#### 2. Methods

#### 2.1. Observations

To answer the previous questions, this study employs several winter observations of sea ice, snow, and near-surface atmosphere collected during the MOSAiC expedition. Direct sea ice measurements include repeated transect surveys that characterized separately the sea ice and snow thickness (respectively  $h_i$  and  $h_s$ ) for multiple in-line locations at the MOSAiC central observatory (Itkin et al., 2023). The spatial resolution of the transect measurements is approximately 1 m. The snow thickness measurements conducted with a depth probe are local and quite precise (uncertainty is <1 cm), while the indirect sea ice thickness measurements rely on a broadband electromagnetic induction sensor and have a larger footprint of up to a few meters, and therefore higher uncertainties (Itkin et al., 2023). During MOSAiC, the ice and snow internal temperatures have been measured with thermistor strings from SIMBA buoys (Lei et al., 2022). Data from buoys 2019T64 and 2019T68 are featured in this study. These measurements provide a high-resolution (2 cm) vertical temperature profile at fixed locations, different from the transects.

Airborne observations were collected during multiple helicopter surveys and provide a two-dimensional (2D) characterization of the snow surface temperature through infrared (IR) camera images (Thielke et al., 2022b) and of the surface elevation through an airborne laser scanner (ALS; Hutter, Hendricks, Jutila, Ricker, et al., 2023). Both products cover a relatively large domain spanning distances of 5–10 km from the MOSAiC central observatory. The surface temperature measurements are derived from broadband infrared brightness temperatures assuming a constant surface emissivity of 0.996. The spatial resolution of the temperature product is approximately 1 m. Temperature measurements are affected by uncertainties that can be larger than 1–2 K. The uncertainty is spatially dependent due to surface emissivity and camera angle variations (Dozier & Warren, 1982). The surface elevation features a resolution of 0.5 m and is converted to snow freeboard based on sea surface height measurements of open leads. Continuous meteorological observations were collected in three distinct locations on the sea ice with a 1-min temporal resolution or less. These include longwave broadband up- and down-welling radiation, downward shortwave radiation, temperature, and wind speed measurements at multiple heights (C. J. Cox, Gallagher, Shupe, Persson, Solomon, et al., 2023). Thielke et al. (2024) includes a validation of the airborne IR temperatures against the ground-based meteorological observations.

Since the airborne and transect observations were collected at different times and processed by multiple providers, a co-location procedure is needed to use them together and ensure that the correct conclusions are drawn from the data. In particular, the ALS freeboard measurements serve as a bridge product to co-locate the helicopter IR surface temperature and the transects. First, we co-locate the IR temperature on top of the ALS snow freeboard by matching thermal and elevation signals of refrozen leads and ridges. Second, we drift-correct the transects based on the ice movement to match the ALS freeboard in time and space and consequently, also the surface temperature. The readers should note that the reference coordinates and times adopted in the paper refer to the airborne survey and not to the matched drift-corrected transect. Dates in the manuscript follow the YYYY.MM. DD convention. To ensure high-quality observations, we consider only transects measured within 2 days from the helicopter flights to avoid position errors due to sea ice deformation. Furthermore, transects in proximity to major snowfall and high-wind events are discarded since these could change the surface topography and decrease their agreement with airborne surveys.

#### 2.2. Model Configuration

To study the impact of the small-scale heterogeneity and horizontal heat conduction on the conductive heat flux computations, we solve the 2D heat equation for multiple MOSAiC transects using a finite element (FE) framework similar to Clemens-Sewall et al. (2024). This approach leads to estimating the equilibrium temperature within sea ice and snow (more details in Text S1 in Supporting Information S1). Each transect undergoes an unstructured-mesh tessellation so that the domain is numerically discretized with an approximate spatial resolution of 10 cm, with local mesh resolution refinements to tessellate regions with snow depth lower than 10 cm.

ZAMPIERI ET AL. 3 of 11

Except for the FE formulation, our model follows all the assumptions made in the standard configuration of the Icepack sea ice single-column model (Hunke, Allard, Bailey, Blain, Craig, Dupont, & Winton, 2022), the thermodynamic component of CICE (Hunke, Allard, Bailey, Blain, Craig, Dupont, & Worthen, 2022), widely used both for sea ice forecasting and climate modeling (Roberts et al., 2018). The thermal conductivity of sea ice  $(k_i)$  is set to 2.1 W m<sup>-1</sup> K<sup>-1</sup>, and  $k_i$  to 0.3 W m<sup>-1</sup> K<sup>-1</sup>, with the latter perturbed in certain sensitivity experiments. In reality,  $k_i$  is temperature and salinity dependent, an aspect that can lead to deviations from the assumed value particularly for newly formed ice close to the ice-ocean interface. The atmospheric heat fluxes used as model boundary conditions (BCs) are directly prescribed from observations in the case of the downward longwave and shortwave radiation fluxes. In the case of the sensible and latent heat fluxes, BCs are derived from the surface temperature, atmospheric 2 m temperature, and 2 m relative humidity following the Monin-Obukhov similarity theory. A broadband albedo of 0.85 is prescribed for the snow (relevant only for two spring flights). The surface emissivity is set to 0.996 for consistency with the retrieval of the airborne surface temperature. Finally, the oceansea ice interface temperature is set to the sea ice melting temperature via Dirichlet BC to simplify the problem, but we acknowledge the availability of oceanic MOSAiC observations (Schulz et al., 2023). The partial differential equation is solved with the DOLFINx Python package, the problem-solving environment of the FEniCSx computing platform (Scroggs, Baratta, et al., 2022; Scroggs, Dokken, et al., 2022).

#### 3. Results

#### 3.1. Impact of Unresolved Thickness Heterogeneity and Horizontal Heat Conduction

Figure 1a displays the snow and sea ice thickness for a transect measured within 48 hr from 16 January 2020 (*Nloop* in Itkin et al. (2023)). The sea ice appears highly deformed, with multiple ridges up to 8 m thick. The snow also shows substantial heterogeneity, mostly driven by the wind redistribution onto the heterogeneous ice surface. Here, we depict the sea ice-snow interface (IS) as a flat line, but in reality, its elevation varies following the hydrostatic balance of the system. Figure 1b depicts the same transect but discretized based on the standard ITD classes of the CICE model. Comparing these two plots reveals that most of the original small-scale heterogeneity is lost by the numerical discretization.

Figures 1c and 1d show the temperature solution of the FE thermodynamic model respectively for the 1D (vertical) and the 2D (vertical and horizontal) heat conduction at different locations within or at the boundaries of the sea ice and snow. The surface equilibrium temperature  $T_{SA}$  shows only small fluctuations and it is within the uncertainty range of the helicopter observations  $T_{SA \ Obs}$ . Most of the temperature variations along the transect can be seen at the IS interface and it is driven by both the sea ice and snow thickness variations. Specifically, the following three mechanisms can explain, to a certain extent, IS temperature variations:

- 1. When thick and therefore insulating snow is found on relatively thin ice, the heat dissipation at the surface is inhibited and heat from the ocean is conducted effectively to the IS interface.
- 2. In the case of thick sea ice, the IS interface is effectively insulated by the ice below and reaches a cooler equilibrium temperature. The insulating effect of the snow layer is less relevant in this situation.
- 3. Regions of thin snow surrounded by thick snow are characterized by strong heat conduction and lead to a cooler  $T_{IS}$  and warmer  $T_{SA}$ .

Overall, we find it remarkable that up to 20 K horizontal temperature fluctuations occur within the simulated system over distances less than 100 m. At the same time, the surface and bottom interface temperatures remain mostly constant because they are heavily influenced by the atmospheric and oceanic state. Compared to the 1D conduction case, the 2D solution shows more spatial variability at the snow-air interface, because thin snow regions can collect heat also from the surrounding ice and dissipate it through surface hot spots. On the contrary, the interior of the ice and snow becomes more uniform in the 2D case because the horizontal heat redistribution tends to homogenize thickness-driven temperature differences. The length scale of horizontal fluxes is variable but typically small, at most a few meters within the ice.

Figure 2a shows the conductive heat flux difference between the 1D vertical thermodynamic solution that resolves the small-scale thickness heterogeneity and the average ITD discretized solution (1D-1D<sub>ITD</sub>; y-axis), as a function of the conductive heat flux average ITD discretized solution (x-axis). Results from all the available transect simulations collected during MOSAiC and following the criteria exposed in Section 2.1 are combined in Figure 2 and indicated with different colors. These transects include but are not limited to the *NLoop* in Figure 1.

ZAMPIERI ET AL. 4 of 11

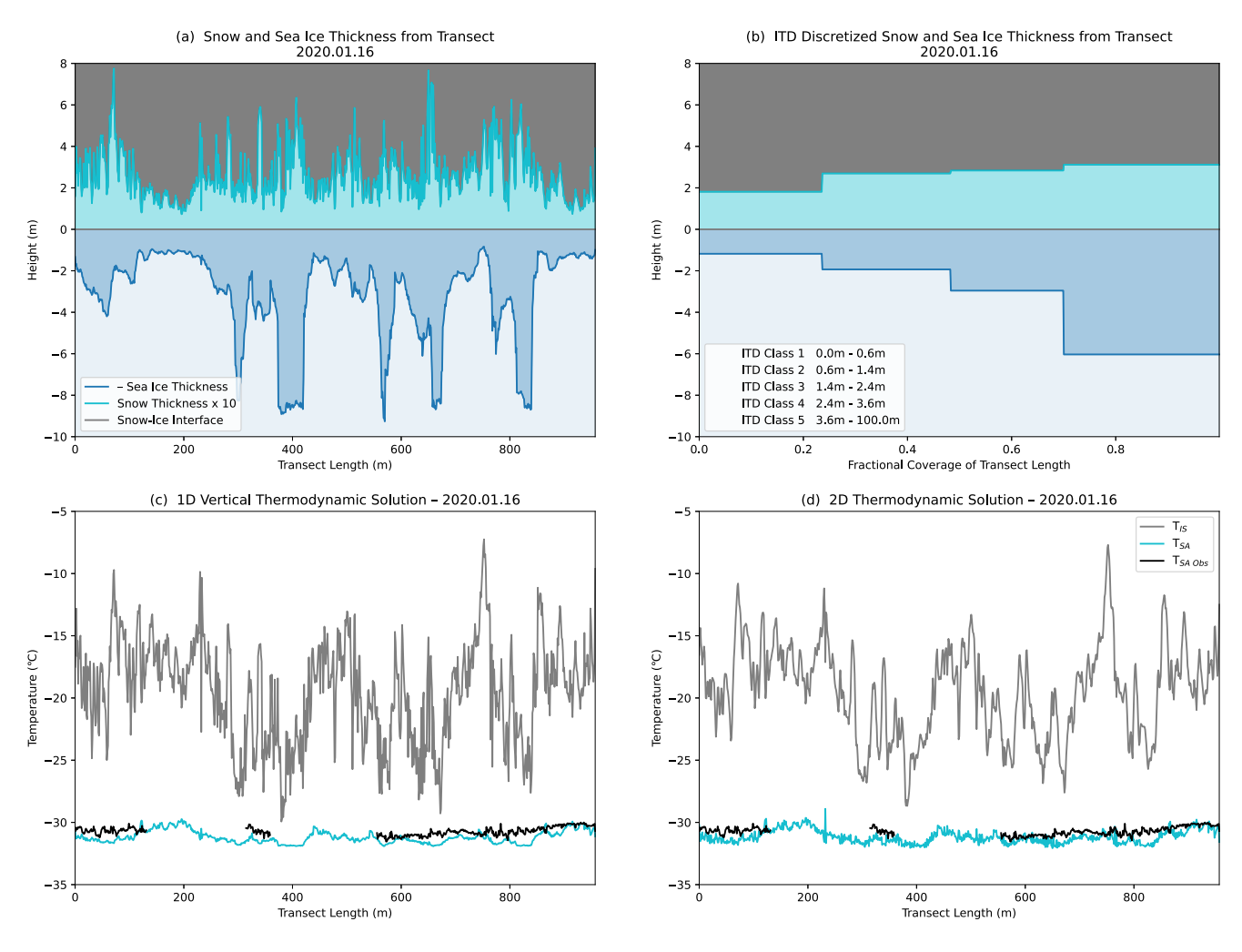


Figure 1. (a): Representation of the sea ice and snow thickness for the *Nloop* transect co-located onto the 16 January 2020 helicopter flight. The snow thickness is magnified by a 10× factor to improve readability. The ice thickness is negative to depict a more realistic configuration with snow above the sea ice. Panel (b) same as panel (a), but discredited into 5 Ice Thickness Distribution classes following the model formulation. Note that Class 1 is absent because the ice is not thin enough in this example. (c, d) Transect temperature profiles at different vertical levels for the 1D vertical and 2D model setups. SA = snow-atmosphere interface, IS = ice-snow interface.

In Figure 2, different symbols refer to the five ITD classes. The result indicates that solving the sea ice and snow thermodynamic without taking into account the small-scale heterogeneity leads to an underestimation of winter heat conduction of up to 10% given the prescribed snow and sea ice conductivity values ( $k_i = 2.1 \text{ W m}^{-1} \text{ K}^{-1}$  and  $k_s = 0.3 \text{ W m}^{-1} \text{ K}^{-1}$ ). The underestimation is proportional to the conductive heat flux itself and therefore marked for ITD classes 1 and 2 ( $\Delta F_{Cond} \approx -1.6 \text{ W m}^{-2}$ ) and small for ITD classes 3 to 5 ( $\Delta F_{Cond} \approx -0.5 \text{ W m}^{-2}$ ).

When solving the heat equation by taking into account horizontal heat conduction in addition to the small-scale heterogeneity (Figure 2b; 2D-1D $_{ITD}$ ), we observe an overall increase of the heat conduction underestimation for high-fraction sea ice classes (larger markers) because the thin snow part of the domain can now dissipate heat from the surrounding ice. We performed a linear fit to the data weighted by the accumulated number of points considered in each estimate, and the increase of the linear fit slope (LFS) from  $2.7 \times 10^{-2}$  to  $6.5 \times 10^{-2}$  quantitatively confirms this behavior. Nevertheless, the signal of low-fraction sea ice classes (smaller markers) is noisier and, in certain instances, even points to an overestimation of the heat conduction by the ITD model in the 2D case.

The importance of horizontal heat conduction grows for more insulating snow, assuming an identical sea ice thermal conductivity. This behavior is reasonable: the more we insulate the surface vertically, the more horizontal dissipation pathways are preferred, and ultimately hot spots associated with thin snow can collect heat from

ZAMPIERI ET AL. 5 of 11

19448007, 2024, 8, Downloaded from https://agupubs.onlinelibrary.wiley.com/doi/10.1029/2023GL106760 by National Center for Atmospheric Research, Wiley Online Library on [18/12/2024]. See the Terms and Conditions

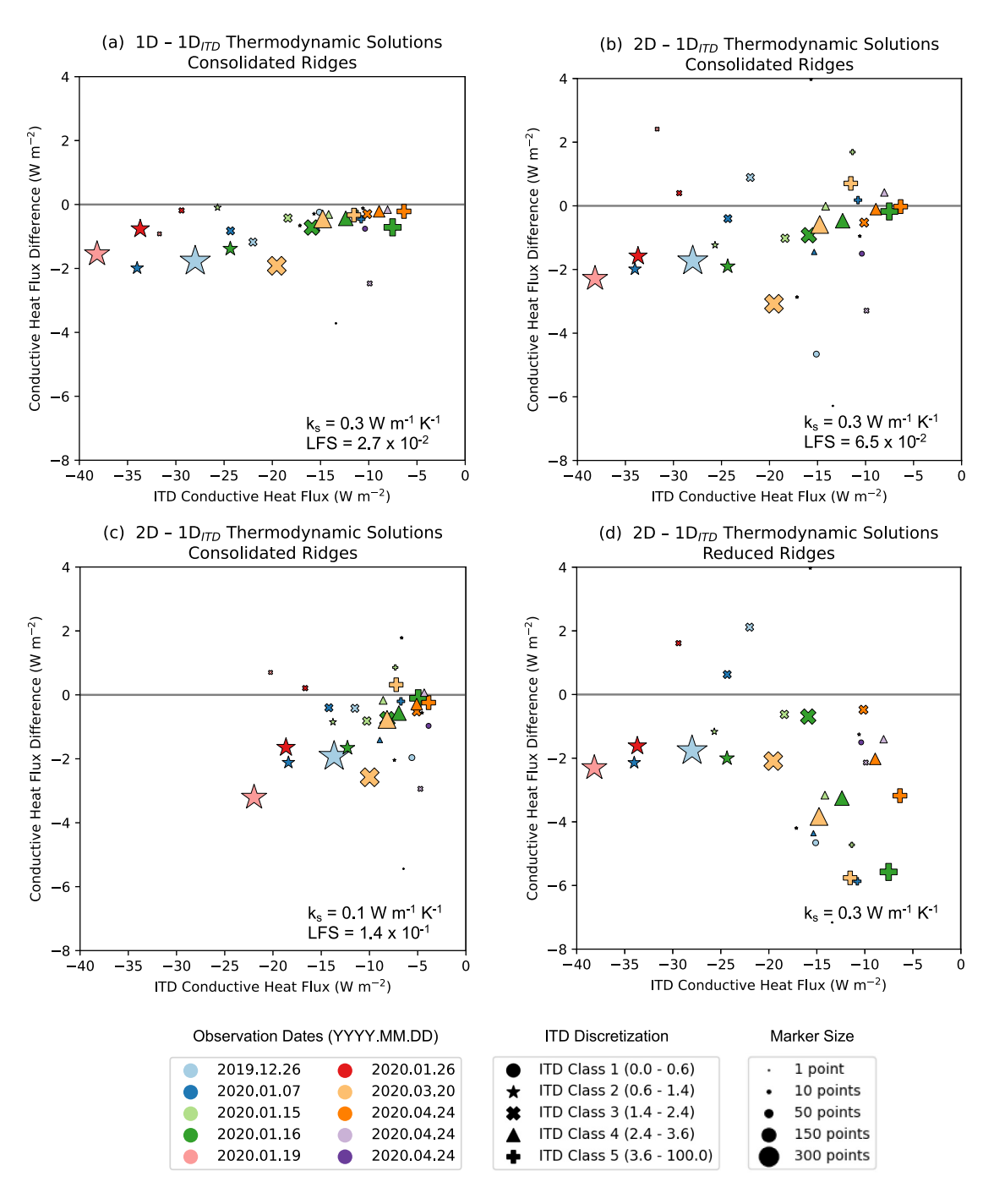


**Figure 2.** (a) Conductive heat flux difference between the 1D vertical thermodynamic solution fully resolving the ice and snow thickness heterogeneity and the 1D solution for the CICE Ice Thickness Distribution (ITD) discretization as a function of the heat flux of the ITD discretization. Panel (b) is similar to panel (a), but with both vertical and horizontal heat conduction (2D) are considered. Panel (c) is similar to panel (b), but for a lower snow thermal conductivity ( $k_s$ ). Panel (d) is similar to panel (b), but the thermodynamic thickness of ridges has been reduced in the 2D solution for representing non-consolidated deformed ice. The size of the markers scales with the accumulated number of points considered in each estimate. LFS = Linear Fit Slope (not computed for d).

portions of the domain further away. This is evident from Figure 2c, where decreasing  $k_s$  to  $k_s = 0.1 \text{ W m}^{-1} \text{ K}^{-1}$  diminishes the magnitude of the heat conduction compared to Figure 2b while simultaneously increasing the underestimation of conduction by a factor of two (LFS =  $1.4 \times 10^{-1}$ ). We would like to point out that  $k_s = 0.1 \text{ W m}^{-1} \text{ K}^{-1}$  is chosen for performing a sensitivity test in line with Sturm, Perovich, and Holmgren (2002),

ZAMPIERI ET AL. 6 of 11

but that such a low value is outside the MOSAiC observational range for this column integrated parameter (Macfarlane, Löwe, et al., 2023).

Previously, we followed the typical model assumptions and represented deformed ice as fully consolidated. In reality, the bottom portion of sea ice ridges features water-filled voids (Leppäranta et al., 1995; Salganik et al., 2023). Hence, no heat conduction occurs within nonconsolidated deformed ice but only in the fully frozen part, which exhibits a thickness ratio to the surrounding level ice of 1.4–1.8 (Høyland, 2002). For more realistic results, we have reduced the thermodynamic thickness of ridges following a simple approach described in Text S2 and Figure S1 in Supporting Information S1 and repeated our simulations. Specifically, we assume a spatially constant ridged-to-level ice ratio of 1.5 for all the deformed ice in the transects. The outcome is displayed in Figure 2d. Compared to Figure 2b, deformed ice (ITD classes 4 and 5) becomes much more conducive, while the conduction of class-3 ice, which typically surrounds ridges, is slightly reduced. Ice in classes 1 and 2 show no noticeable change. Overall, the ITD solution in Figure 2d underestimates the conductive heat flux for most of the sea ice in the transects.

Finally, we briefly discuss whether the horizontal heat conduction is stronger within the sea ice or snow. Figure S2 in Supporting Information S1 shows that the horizontal component of the flux is larger in the sea ice, which is reasonable given its higher thermal conductivity. Interestingly, the same plot suggests there is not a strong dependence of the horizontal flux on the thickness of ice and snow, but it rather appears that the horizontal fluxes are just slightly stronger over the thinner part of the domain. Similar results hold for the case with reduced ridges (Figure S2d in Supporting Information S1).

#### 3.2. Testing Snow Conductivity Tuning Under Process-Oriented Diagnostics

In the previous paragraphs, we showed a reasonable agreement between the simulated and observed surface temperature for the transect under consideration (Figure 1c; 16 January 2020 simulation). However, this holds only for the thick ice cover, while a positive temperature bias emerges for thin ice and snow, meaning that the simulated surface temperature is warmer than the observations. For example, the transect measured on first-year ice on 7 January 2020 (Dark FYI in Itkin et al. (2023)) had a considerable amount of thin ice (Figure 3c) and comparisons of the simulated surface temperature to observations (Figure 3a) show large discrepancies in these regions. Different mechanisms could explain this positive temperature bias: (a) An overestimation of the thermal conductivity of sea ice and snow would cause excessive conduction through the sea ice system, or (b) An erroneous computation of the turbulent and radiative energy fluxes at the surface. Here we test the first hypothesis by reducing the simulated snow thermal conductivity, which should mitigate the positive surface bias. Specifically, we repeat the simulation by decreasing the snow conductivity from a value of 0.3 W m<sup>-1</sup> K<sup>-1</sup> (Figures 3a) to 0.1 W m<sup>-1</sup> K<sup>-1</sup> (Figure 3b), and we observe a substantial reduction from 2.55 to 1.14 K of the surface temperature bias. Note that a residual error is inevitable and thus expected given the time difference of up to 2 days between the flights and the transect survey, during which ice growth, deformation, and more importantly snow redistribution compaction could occur. Admittedly, a k<sub>s</sub> value of 0.1 W m<sup>-1</sup> K<sup>-1</sup> is physically plausible but not compatible with the direct observations of this parameter during MOSAiC (Macfarlane, Löwe, et al., 2023). Nonetheless, performing such sensitivity simulation is informative for the modeling community, which routinely uses  $k_s$  as a tuning parameter as explained in Section 1. In the next paragraph, we will investigate whether this bias reduction linked to the tuning of  $k_r$  holds when tested in the context of thermodynamic-oriented diagnostics.

Tuning the snow conductivity has strong implications also for the temperature within sea ice and snow. Given that the simulated snow becomes a stronger insulator, less heat is fluxed from the ice through the snow and so more heat is retained within the sea ice, leading to a warming of approximately 7 K at the interface of the ice and snow. We tested whether this new temperature structure, which leads to a surface bias reduction, is also reasonable when compared to observations of the sea ice and snow interior. Figure 3d exhibits the sea ice temperature gradient at half of the sea ice thickness as a function of the effective thermodynamic thickness  $h_e$ , a quantity often used by sea ice modelers defined as  $h_e = h_i + h_s \frac{k_i}{k_i}$ . For both the conductivity values, we observe that the temperature gradient decreases as the thickness increases. This behavior agrees well with our understanding of the system, as thicker sea ice provides more thermal insulation and tends to host, on average, thicker snow. However, a comparison with independent measurements from the SIMBA buoys reveals that the sea ice thermal structure emerging from the simulation with a snow thermal conductivity of 0.3 W m<sup>-1</sup> K<sup>-1</sup> (cyan markers) agrees better with the SIMBA

ZAMPIERI ET AL. 7 of 11

19448007, 2024, 8, Downloaded from https://agupubs.onlinelibrary.wiley.com/doi/10.1029/2023GL106760 by National Center for Atmospheric Research, Wiley Online Library on [18/12/2024]. See the Terms and Conditions (https://

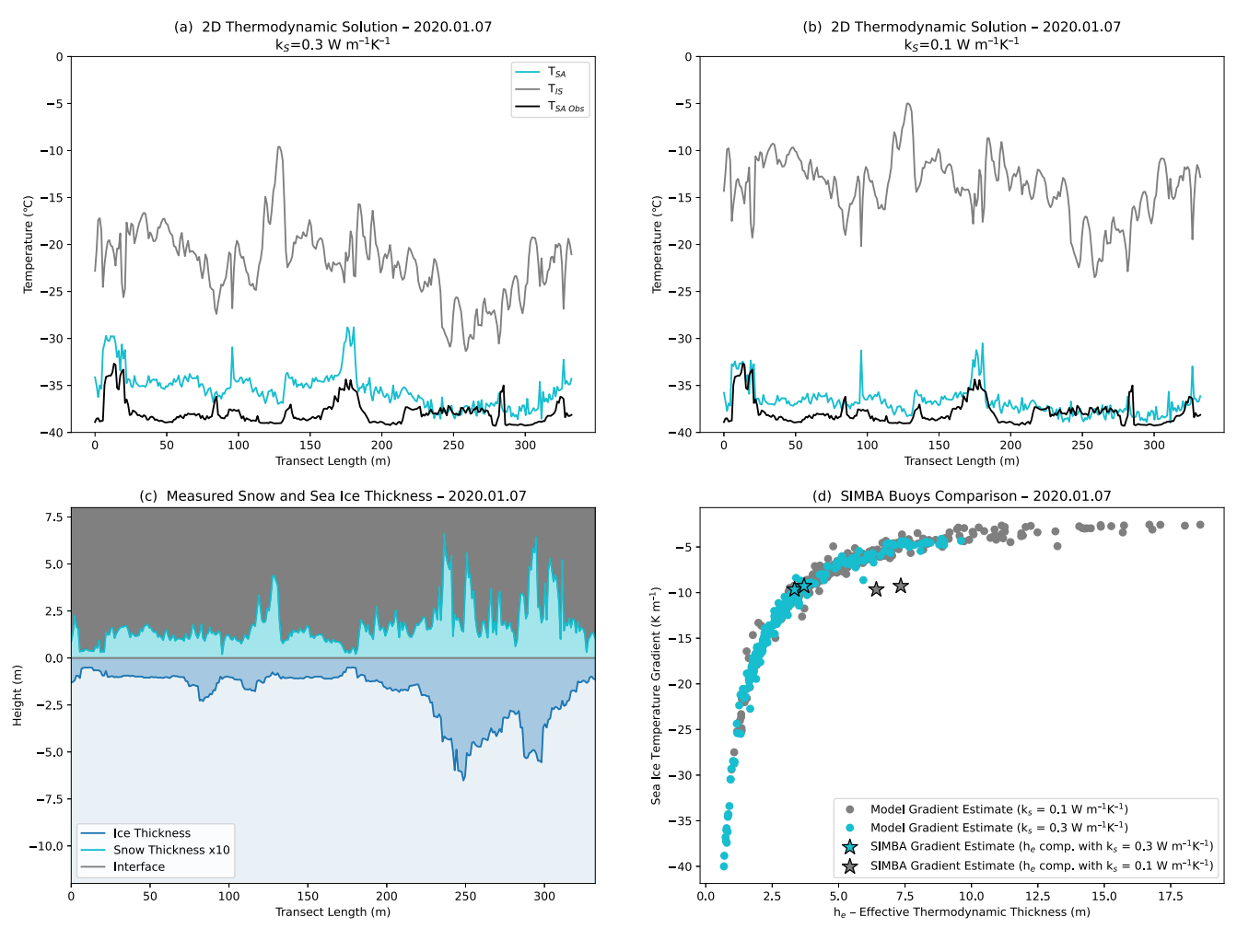


Figure 3. (a, b) Transect temperature profiles at different vertical levels for two different snow thermal conductivity values. (c) Representation of the sea ice and snow thickness for the *Dark FYI* transect co-located onto the 7 January 2020 helicopter flight. The snow thickness is magnified by a factor  $10 \times$  to improve readability. The ice thickness is negative to depict a more realistic configuration with snow above the sea ice. (d): Simulated temperature gradient at half of the sea ice thickness for two different snow conductivity values compared to two SIMBA measurements as a function of the effective thermodynamic ice thickness  $h_e$ . SA = snow-atmosphere interface, IS = ice-snow interface.

observations. Based on this, attributing the surface temperature bias solely to an erroneous representation of the conduction appears problematic, meaning that the surface flux computation likely plays a major role.

#### 4. Discussion and Conclusions

Our results reveal that a model formulation that does not take into account the meter-scale sea ice and snow thickness heterogeneity and the horizontal heat conduction processes tends to underestimate the winter heat conduction by approximately 10% for the standard set of thermodynamic parameters in a well-used sea ice model. In this respect, our result agrees with the findings of Sturm, Perovich, and Holmgren (2002), although they simulate a much larger impact with an underestimation of 40%. This difference can be in part explained if considering that the snow thermal conductivity used in Sturm, Perovich, and Holmgren (2002) was 0.14 W m<sup>-1</sup> K<sup>-1</sup>, approximately half of that of our simulations. As we mentioned above, the importance of horizontal heat conduction processes tends to grow as the snow becomes more insulating. Another reason for this discrepancy might be related to the substantially higher amount of observations available for MOSAiC, and thus considered in our study. MOSAiC transects span both level and deformed ice covered by a very heterogeneous snow layer, while the 40 m Seattle transect of Sturm, Perovich, and Holmgren (2002) is limited to refrozen ponded ice covered by thick snow and ice hummocks with little snow.

ZAMPIERI ET AL. 8 of 11



Acknowledgments

As part of the Virtual Earth System Research Institute (VESRI), funding for

the Multiscale Machine Learning In coupled Earth System Modeling

supported by the European Union's

program under grant agreement no. 101003826 via the project CRiceS

(Climate Relevant interactions and

feedbacks: the key role of sea ice and Snow in the polar and global climate system). D. C-S. was supported by the NSF award 2138788. A.S. was supported by the DOE

Atmospheric System Research Program

(DE-SC0021341) and in part by NOAA

NA22OAR4320151. N.H was funded by the Cooperative Institute for Climate,

Ocean, & Ecosystem Studies (CICOES)

under NOAA Cooperative Agreement NA20OAR4320271, Contribution No.

2024-1336, and by the German Federal Ministry of Education and Research

(BMBF) project IceSense-Remote

Sensing of the Seasonal Evolution of

(03F0866A). Observations used here from the MOSAiC 2019/2020 expedition were

Measurement (ARM) User Facility, a U.S. Department of Energy (DOE) Office of

Science User Facility Managed by the Biological and Environmental Research

Program. Finally, we are thankful for the

anonymous reviewers and to Dr. Martin

Vancoppenolle for his precious feedback.

insightful comments received by two

Climate-relevant Sea Ice Properties

made by the Atmospheric Radiation

cooperative agreement

Horizon 2020 research and innovation

(M<sup>2</sup>LInES) project was provided to L.Z. and M.H. by the generosity of Eric and

Wendy Schmidt by recommendation of the Schmidt Futures program. L.Z. was also

### **Geophysical Research Letters**

10.1029/2023GL106760

Assessing whether these unresolved processes ultimately matter for the sea ice mass balance and have relevance for the polar climate requires their parameterization in climate models, which goes beyond the scope of this study and will be conducted in future work. While accurately modeling the conduction within the sea ice system is important both for level and deformed sea ice, our study also reveals that the chosen parameterization of the radiative and turbulent surface fluxes presents shortcomings that lead to substantial surface temperature biases. This aspect should also be addressed when developing sea ice models, as the benefit of improved conduction will diminish if the surface processes are incorrectly represented. In fact, simpler surface heat budget parameterizations (Maykut, 1986) appear to perform better in the context of MOSAiC observations (Shupe et al., 2022). Moreover, the heat conduction model underestimation for ridges evidenced by our work calls for additional efforts for describing deformed sea ice processes not only mechanically (Hutter et al., 2019; Roberts et al., 2018) but also thermodynamically (Leppäranta et al., 1995; Salganik et al., 2021).

Our analyses focus primarily on process-oriented diagnostics rather than large-scale metrics for assessing the quality of simulations. Considering that the insulating role of snow on sea ice is often overlooked or extremely simplified in modeling (Arduini et al., 2022; Batrak & Müller, 2019; Zampieri et al., 2023), we believe a process-oriented approach to be the key to stepping forward in the sea ice model development field, and we call for applying this protocol in future model development initiatives. Not only do we want models that simulate a convincing large-scale sea ice state, but we also want the processes and feedback mechanisms to be as correct as possible. Only under these conditions model predictions and projections can be trusted and meaningful adaptation strategies can be designed. Furthermore, this study demonstrates the importance of an in-depth model evaluation based on observations from multiple sources. In this respect, the use of the observational data set generated from MOSAiC in its entirety has great potential to guide the sea ice model development efforts in the upcoming years in the context of a fast-changing Arctic sea ice cover. By addressing these challenges and refining our models, we can aim to provide more accurate predictions about the current state and future evolution of sea ice, especially in the context of ongoing global warming. Improved representations of thermodynamic processes in sea ice models will contribute to a better understanding of the Arctic climate system and its response to environmental changes.

#### **Data Availability Statement**

The datasets used in this study are all freely accessible, referenced in Section 2.1, and distributed in the following repositories. The IR temperature data can be found in Thielke et al. (2022a). The ALS freeboard data can be found in Hutter, Hendricks, Jutila, Birnbaum, et al. (2023). The transects data can be found in Itkin et al. (2021) and Hendricks et al. (2022). The atmospheric measurements can be found in C. J. Cox, Gallagher, Shupe, Persson, Blomquist, et al. (2023). The Python code used to run the model simulations and reproduce the plots is available on Zenodo (Zampieri, 2023).

#### References

Arduini, G., Keeley, S., Day, J. J., Sandu, I., Zampieri, L., & Balsamo, G. (2022). On the importance of representing snow over sea-ice for simulating the Arctic boundary layer. *Journal of Advances in Modeling Earth Systems*, 14(7), e2021MS002777. https://doi.org/10.1029/2021ms002777

Batrak, Y., & Müller, M. (2019). On the warm bias in atmospheric reanalyses induced by the missing snow over Arctic sea-ice. *Nature Communications*, 10(1), 4170. https://doi.org/10.1038/s41467-019-11975-3

Clemens-Sewall, D., Polashenski, C., Perovich, D., & Webster, M. A. (2024). The importance of sub-meter-scale snow roughness on conductive heat flux of Arctic sea ice. *Journal of Glaciology*, 1–17. https://doi.org/10.1017/jog.2023.105

neat flux of Arctic sea ice. *Journal of Glaciology*, 1–17. https://doi.org/10.101//jog.2023.105

Clemens-Sewall, D., Smith, M. M., Holland, M. M., Polashenski, C., & Perovich, D. (2022). Snow redistribution onto young sea ice: Observations and implications for climate models. *Elementa: Science of the Anthropocene*, 10(1), 00115. https://doi.org/10.1525/elementa.2021.00115

Cox, C. J., Gallagher, M., Shupe, M., Persson, O., Blomquist, B., Grachev, A., et al. (2023). Met city meteorological and surface flux measurements (level 2 processed), multidisciplinary drifting observatory for the study of arctic climate (MOSAiC), central arctic, October 2019–September 2020 [Dataset]. NSF Arctic Data Center. https://doi.org/10.18739/A2TM7227K

Cox, C. J., Gallagher, M. R., Shupe, M. D., Persson, P. O. G., Solomon, A., Fairall, C. W., et al. (2023). Continuous observations of the surface energy budget and meteorology over the Arctic sea ice during MOSAiC. *Scientific Data*, 10(1), 519. https://doi.org/10.1038/s41597-023-02415-5

Dozier, J., & Warren, S. G. (1982). Effect of viewing angle on the infrared brightness temperature of snow. Water Resources Research, 18(5), 1424–1434. https://doi.org/10.1029/wr018i005p01424

Fichefet, T., & Maqueda, M. A. M. (1997). Sensitivity of a global sea ice model to the treatment of ice thermodynamics and dynamics. *Journal of Geophysical Research*, 102(C6), 12609–12646. https://doi.org/10.1029/97jc00480

Hendricks, S., Itkin, P., Ricker, R., Webster, M., von Albedyll, L., Rohde, J., et al. (2022). GEM-2 quicklook total thickness measurements from the 2019–2020 MOSAiC expedition [Dataset]. PANGAEA. https://doi.org/10.1594/PANGAEA.943666

Holland, M. M., Bitz, C. M., & Tremblay, B. (2006). Future abrupt reductions in the summer Arctic sea ice. Geophysical Research Letters, 33(23), L23503. https://doi.org/10.1029/2006g1028024

ZAMPIERI ET AL. 9 of 11

- Høyland, K. V. (2002). Consolidation of first-year sea ice ridges. *Journal of Geophysical Research*, 107(C6), 15-1. https://doi.org/10.1029/2000jc000526
- Hunke, E., Allard, R., Bailey, D. A., Blain, P., Craig, A., Dupont, F., et al. (2022). CICE-consortium/icepack: Icepack 1.3.3. Zenodo. https://doi.org/10.5281/ZENODO.7419438
- Hunke, E., Allard, R., Bailey, D. A., Blain, P., Craig, A., Dupont, F., et al. (2022). CICE-consortium/CICE: CICE version 6.4.1. Zenodo. https://doi.org/10.5281/ZENODO.7419531
- Hutter, N., Hendricks, S., Jutila, A., Birnbaum, G., von Albedyll, L., Ricker, R., & Haas, C. (2023). Merged grids of sea-ice or snow freeboard from helicopter-borne laser scanner during the MOSAiC expedition, version 1 [Dataset]. PANGAEA. https://doi.org/10.1594/PANGAEA.050806
- Hutter, N., Hendricks, S., Jutila, A., Ricker, R., von Albedyll, L., Birnbaum, G., & Haas, C. (2023). Digital elevation models of the sea-ice surface from airborne laser scanning during mosaic. *Scientific Data*, 10(1), 729. https://doi.org/10.1038/s41597-023-02565-6
- Hutter, N., Zampieri, L., & Losch, M. (2019). Leads and ridges in arctic sea ice from RGPS data and a new tracking algorithm. *The Cryosphere*, 13(2), 627–645. https://doi.org/10.5194/tc-13-627-2019
- Itkin, P., Hendricks, S., Webster, M., von Albedyll, L., Arndt, S., Divine, D., et al. (2023). Sea ice and snow characteristics from year-long transects at the MOSAiC central observatory. *Elementa: Science of the Anthropocene*, 11(1), 00048. https://doi.org/10.1525/elementa.2022.
- Itkin, P., Webster, M., Hendricks, S., Oggier, M., Jaggi, M., Ricker, R., et al. (2021). Magnaprobe snow and melt pond depth measurements from the 2019–2020 MOSAiC expedition [Dataset]. PANGAEA. https://doi.org/10.1594/PANGAEA.937781
- Jutila, A., Hendricks, S., Ricker, R., von Albedyll, L., Krumpen, T., & Haas, C. (2022). Retrieval and parameterisation of sea-ice bulk density from airborne multi-sensor measurements. The Cryosphere, 16(1), 259–275. https://doi.org/10.5194/tc-16-259-2022
- Landrum, L. L., & Holland, M. M. (2022). Influences of changing sea ice and snow thicknesses on simulated Arctic winter heat fluxes. The Cryosphere, 16(4), 1483–1495. https://doi.org/10.5194/tc-16-1483-2022
- Lecomte, O., Fichefet, T., Vancoppenolle, M., Domine, F., Massonnet, F., Mathiot, P., et al. (2013). On the formulation of snow thermal conductivity in large-scale sea ice models. *Journal of Advances in Modeling Earth Systems*, 5(3), 542–557. https://doi.org/10.1002/jame.20039
- Lei, R., Cheng, B., Hoppmann, M., Zhang, F., Zuo, G., Hutchings, J. K., et al. (2022). Seasonality and timing of sea ice mass balance and heat fluxes in the Arctic transpolar drift during 2019–2020. *Elementa: Science of the Anthropocene*, 10(1), 000089. https://doi.org/10.1525/elementa.2021.000089
- Leppäranta, M., Lensu, M., Kosloff, P., & Veitch, B. (1995). The life story of a first-year sea ice ridge. Cold Regions Science and Technology, 23(3), 279–290. https://doi.org/10.1016/0165-232x(94)00019-t
- Lipscomb, W. H. (2001). Remapping the thickness distribution in sea ice models. Journal of Geophysical Research, 106(C7), 13989–14000. https://doi.org/10.1029/2000jc000518
- Macfarlane, A. R., Löwe, H., Gimenes, L., Wagner, D. N., Dadic, R., Ottersberg, R., et al. (2023). Thermal conductivity of snow on Arctic sea ice. https://doi.org/10.5194/egusphere-2023-83
- Macfarlane, A. R., Schneebeli, M., Dadic, R., Tavri, A., Immerz, A., Polashenski, C., et al. (2023). A database of snow on sea ice in the central Arctic collected during the MOSAiC expedition. *Scientific Data*, 10(1), 398. https://doi.org/10.1038/s41597-023-02273-1
- Mårtensson, S., Meier, H. E. M., Pemberton, P., & Haapala, J. (2012). Ridged sea ice characteristics in the Arctic from a coupled multicategory sea ice model. *Journal of Geophysical Research*, 117(C8), C00D15. https://doi.org/10.1029/2010jc006936
- Massonnet, F., Barthélemy, A., Worou, K., Fichefet, T., Vancoppenolle, M., Rousset, C., & Moreno-Chamarro, E. (2019). On the discretization of the ice thickness distribution in the NEMO3.6-LIM3 global ocean–sea ice model. Geoscientific Model Development, 12(8), 3745–3758. https:// doi.org/10.5194/gmd-12-3745-2019
- Maykut, G. A. (1986). The surface heat and mass balance. In *The geophysics of sea ice* (pp. 395–463). Springer US. https://doi.org/10.1007/978-1-4899.5352-0-6
- Nicolaus, M., Perovich, D. K., Spreen, G., Granskog, M. A., von Albedyll, L., Angelopoulos, M., et al. (2022). Overview of the MOSAiC expedition: Snow and sea ice. *Elementa: Science of the Anthropocene*, 10(1), 000046. https://doi.org/10.1525/elementa.2021.000046
- Perovich, D., Raphael, I., Moore, R., Clemens-Sewall, D., Lei, R., Sledd, A., & Polashenski, C. (2023). Sea ice heat and mass balance measurements from four autonomous buoys during the MOSAiC drift campaign. *Elementa: Science of the Anthropocene*, 11(1), 00017. https://doi.org/10.1525/elementa.2023.00017
- Perovich, D. K., Andreas, E. L., Curry, J. A., Eiken, H., Fairall, C. W., Grenfell, T. C., et al. (1999). Year on ice gives climate insights. *Eos, Transactions American Geophysical Union*, 80(41), 481–486. https://doi.org/10.1029/eo080i041p00481-01
- Petrich, C., Langhorne, P. J., & Haskell, T. G. (2007). Formation and structure of refrozen cracks in land-fast first-year sea ice. *Journal of Geophysical Research*, 112(C4), 6. https://doi.org/10.1029/2006jc003466
- Popović, P., Finkel, J., Silber, M. C., & Abbot, D. S. (2020). Snow topography on undeformed arctic sea ice captured by an idealized "snow dune" model. *Journal of Geophysical Research: Oceans*, 125(9), e2019JC016034. https://doi.org/10.1029/2019jc016034
- Riche, F., & Schneebeli, M. (2013). Thermal conductivity of snow measured by three independent methods and anisotropy considerations. *The Cryosphere*, 7(1), 217–227. https://doi.org/10.5194/tc-7-217-2013
- Roberts, A. F., Hunke, E. C., Allard, R., Bailey, D. A., Craig, A. P., Lemieux, J.-F., & Turner, M. D. (2018). Quality control for community-based sea-ice model development. *Philosophical Transactions of the Royal Society A: Mathematical, Physical & Engineering Sciences*, 376(2129), 20170344. https://doi.org/10.1098/rsta.2017.0344
- Salganik, E., Høyland, K. V., & Shestov, A. (2021). Medium-scale experiment in consolidation of an artificial sea ice ridge in van Mijenfjorden, Svalbard. Cold Regions Science and Technology, 181, 103194. https://doi.org/10.1016/j.coldregions.2020.103194
- Salganik, E., Lange, B. A., Itkin, P., Divine, D., Katlein, C., Nicolaus, M., et al. (2023). Different mechanisms of arctic first-year sea-ice ridge consolidation observed during the mosaic expedition. https://doi.org/10.31223/x52082
- Schulz, K., Koenig, Z., Muilwijk, M., Bauch, D., Hoppe, C. J. M., Droste, E., et al. (2023). The Eurasian Arctic Ocean along the MOSAiC drift (2019–2020): An interdisciplinary perspective on properties and processes. https://doi.org/10.31223/x5tt2w
- Schwerdtfecer, P. (1963). The thermal properties of sea ice. *Journal of Glaciology*, 4(36), 789–807. https://doi.org/10.3189/s0022143000028379
  Scroggs, M. W., Baratta, I. A., Richardson, C. N., & Wells, G. N. (2022). Basix: A runtime finite element basis evaluation library. *Journal of Open Source Software*, 7(73), 3982. https://doi.org/10.21105/joss.03982
- Scroggs, M. W., Dokken, J. S., Richardson, C. N., & Wells, G. N. (2022). Construction of arbitrary order finite element degree-of-freedom maps on polygonal and polyhedral cell meshes. ACM Transactions on Mathematical Software, 48(2), 1–23. https://doi.org/10.1145/3524456
- Shupe, M. D., Rex, M., Blomquist, B., Persson, P. O. G., Schmale, J., Uttal, T., et al. (2022). Overview of the MOSAiC expedition: Atmosphere. Elementa: Science of the Anthropocene, 10(1), 54. https://doi.org/10.1525/elementa.2021.00060

ZAMPIERI ET AL. 10 of 11

- Sturm, M., Holmgren, J., König, M., & Morris, K. (1997). The thermal conductivity of seasonal snow. *Journal of Glaciology*, 43(143), 26–41. https://doi.org/10.3189/s0022143000002781
- Sturm, M., Holmgren, J., & Perovich, D. K. (2002). Winter snow cover on the sea ice of the Arctic Ocean at the surface heat budget of the arctic ocean (SHEBA): Temporal evolution and spatial variability. *Journal of Geophysical Research*, 107(C10), 23. https://doi.org/10.1029/2000jc000400
- Sturm, M., Perovich, D. K., & Holmgren, J. (2002). Thermal conductivity and heat transfer through the snow on the ice of the Beaufort Sea. Journal of Geophysical Research, 107(C10), 8043. https://doi.org/10.1029/2000jc000409
- Thielke, L., Huntemann, M., Hendricks, S., Jutila, A., Ricker, R., & Spreen, G. (2022a). Helicopter-borne thermal infrared sea ice surface temperatures during the MOSAiC expedition, version 2 [Dataset]. PANGAEA. https://doi.org/10.1594/PANGAEA.941017
- Thielke, L., Huntemann, M., Hendricks, S., Jutila, A., Ricker, R., & Spreen, G. (2022b). Sea ice surface temperatures from helicopter-borne thermal infrared imaging during the MOSAiC expedition. *Scientific Data*, 9(1), 364. https://doi.org/10.1038/s41597-022-01461-9
- Thielke, L., Spreen, G., Huntemann, M., & Murashkin, D. (2024). Spatio-temporal variability of small-scale leads based on helicopter maps of winter sea ice surface temperatures. *Elementa: Science of the Anthropocene*, 12(1), 40. https://doi.org/10.1525/elementa.2023.00023
- Thorndike, A. S., Rothrock, D. A., Maykut, G. A., & Colony, R. (1975). The thickness distribution of sea ice. *Journal of Geophysical Research*, 80(33), 4501–4513. https://doi.org/10.1029/jc080i033p04501
- Timco, G., & Frederking, R. (1996). A review of sea ice density. Cold Regions Science and Technology, 24(1), 1–6. https://doi.org/10.1016/0165-232x(95)00007-x
- Urrego-Blanco, J. R., Urban, N. M., Hunke, E. C., Turner, A. K., & Jeffery, N. (2016). Uncertainty quantification and global sensitivity analysis of the Los Alamos sea ice model. *Journal of Geophysical Research: Oceans*, 121(4), 2709–2732. https://doi.org/10.1002/2015ic011558
- von Albedyll, L., Haas, C., & Dierking, W. (2021). Linking sea ice deformation to ice thickness redistribution using high-resolution satellite and airborne observations. *The Cryosphere*, 15(5), 2167–2186. https://doi.org/10.5194/tc-15-2167-2021
- Weeks, W. F., & Assur, A. (1967). The mechanical properties of sea ice. https://doi.org/10.21236/ad0662716
- Zampieri, L. (2023). Izampier/zampieri\_2023\_paper: Postprocessing for "Modelling the winter heat conduction through the sea ice system during MOSAiC" [Software]. Zenodo. https://doi.org/10.5281/zenodo.8414652
- Zampieri, L., Arduini, G., Holland, M., Keeley, S. P. E., Mogensen, K., Shupe, M. D., & Tietsche, S. (2023). A machine learning correction model of the winter clear-sky temperature bias over the Arctic sea ice in atmospheric reanalyses. *Monthly Weather Review*, 151(6), 1443–1458. https://doi.org/10.1175/mwr-d-22-0130.1
- Zampieri, L., Kauker, F., Fröhle, J., Sumata, H., Hunke, E. C., & Goessling, H. F. (2021). Impact of sea-ice model complexity on the performance of an unstructured-mesh sea-ice/ocean model under different atmospheric forcings. *Journal of Advances in Modeling Earth Systems*, 13(5), e2020MS002438. https://doi.org/10.1029/2020ms002438

ZAMPIERI ET AL. 11 of 11